Assessment of the diagnostics for shape control in fusion machines

Angelo Cenedese Paolo Bettini

Abstract

In fusion devices, the accurate reconstruction of the boundary location and shape from magnetic diagnostics is of paramount importance for the efficient control of the plasma evolution and the safe running of the experiment. In addition to a good and consistent performance in the reconstruction, the task must be performed in real-time as the input for the shape controller and more in general for the scenario optimization. To this aim, a statistical procedure for the evaluation of the reconstruction capability of different magnetic sensor sets is presented, which can drive the choice for an optimal set to be used for the reconstruction of plasma location and boundary shape during real-time operation. In addition, an algorithm to approximately solve the free boundary problem and estimate the plasma shape starting from the magnetics is devised. Beyond representing a first step towards the definition of a boundary reconstruction code for plasma shape control, this tool is also used to cross validate and confirm the statistical analysis on the diagnostics.

I. Introduction

In the context of fusion machines experiments, the research on efficient techniques to guarantee an accurate and real-time reconstruction of the plasma boundary has been a central issue, since such procedures are of paramount importance for both the safe operation of the fusion device and for reaching the expected performance of the designed configuration. The task poses challenges that regard the very nature of the plasma as a deformable magnetic fluid and that relate to the fact that the shape of the plasma or more simply its distance from the facing components are not directly measurable quantities, and need to be inferred from numerous and generally heterogeneous magnetic sensors placed inside and outside the vacuum vessel. In fact, the plasma boundary is defined as the outermost closed flux surface entirely contained in the vacuum chamber, and is then characterized by a specific magnetic flux value.

Assessing the reconstruction capability of the magnetic sensors and highlighting the differences in the reconstruction performance by using different sensor sets are then important tasks that involve modeling and numerical aspects. They also have a direct impact on the control performance both in the selection of the optimal diagnostics combination to ensure efficiency in the reconstruction, and in suggesting the estimation strategy in the regulator design, as the classical integration of observer and controller. In actual fact, the selection of the most significant magnetic signals needs to couple with a proper strategy for the boundary reconstruction that well fits the control scheme adopted for the machine.

Due to the high complexity of the magnetohydrodynamics (MHD) physics and of the experimental devices, where non-linear behaviors of both the plasma and its coupling with the active circuits and the surrounding metallic structures arise, the preliminary validation of diagnostics and control systems is carried out relying on simplified linear models and resorting to extensive numerical simulations [1] in the early stages of the design.

Then, a further evaluation of the magnetic signals and the estimation of derived quantities (such as the plasma boundary location [2]) is assessed during the commissioning phase of the machine, where a set of experiments are run in order to verify and confirm the operational range of the device. In this stage, the cross validation with other measurements for the mere sensor signals, and the comparison with the numerical code simulations for the boundary location and shape reconstruction represent the main tool for sensor assessment [3][4]. Notably, though, the evaluation of the single measurement signal, despite being important for the sensor *per se*, is of limited advantage in the whole reconstruction context, which is the main aim of the diagnostics for control.

Unfortunately, the numerical codes developed for full equilibrium reconstruction from external magnetic measurements [5][6][7] require a severe computational effort hardly suitable for real-time, though some efficient implementations, based on simplifying hypotheses and optimized algorithms, have been proposed [8][9].

In this activity, we will study the magnetic diagnostic system of the ITER machine, in commenced construction stage, with the specific aim of providing guidelines for the design of the control systems, and the more general ambition of setting up a framework for diagnostic analysis and synthesis for other fusion machines and devices where the reconstruction of the magnetic configuration maps is of interest. The contribution of this work is then twofold: On the one side, a methodology to evaluate the reconstruction capability of different magnetic sensor sets is proposed, and the identification of critical issues in the magnetic configuration estimation is provided. On the other side, these issues are key inputs for the design of a real-time boundary reconstruction code, which is a second objective of this activity.

A. Cenedese is with the Department of Information Engineering (DEI), University of Padova, Via Gradenigo 6/B, 35131 Padova, Italy angelo.cenedese@unipd.it. P. Bettini is with the Department of Industrial Engineering (DII), University of Padova, Via Gradenigo 6/A, 35131 Padova, Italy paolo.bettini@unipd.it. Both authors are also with the Fusion Research Center (CRF), University of Padova.

The research leading to these results has been funded by service contract F4E-OPE-349 (PMS-PE) between Fusion for Energy - The European Joint Undertaking for ITER and the Development of Fusion Energy and Consorzio RFX - Associazione Euratom-ENEA per la Fusione. The views and opinions expressed herein do not necessarily reflect those of F4E, nor those of the ITER Organization.

The remainder of the paper is organized as follows: After the description of the machine and some preliminary tools and model in Sec. II, the main contribution is given in Sec. III for the statistical assessment of the sensor sets and in Sec. IV the design of a boundary reconstruction suitable for real-time employment is introduced. Then, in Sec. V the assessment results are presented together with some specific numerical simulations to confirm these findings, and finally in Sec. VI some conclusions are drawn.

II. Description of machine, models and tools

The cross section of the ITER device is shown in Fig. 1(a), highlighting the distribution of magnetic diagnostics on the poloidal plane: The real (designed) sensors are plotted with markers, while a virtual measurement array, located as close as possible to the plasma, is visible as a continuous line partially superimposed on the first wall. In Fig. 1(b), the location of the gap-points and gap-lines for evaluating the plasma-first wall distance during real-time plasma operation are presented. In this regard, two sets are defined: The 6 control gap-lines are used for shape control, meaning that boundary-first wall distances along these lines are given for references and should be computed in real-time and fed-back for shape control; on the other hand, the 24 diagnostics gap-points and gap-lines are a more numerous set used for diagnostics purposes and to control a plasma soft termination in order to avoid the approaching of the plasma to the facing components.

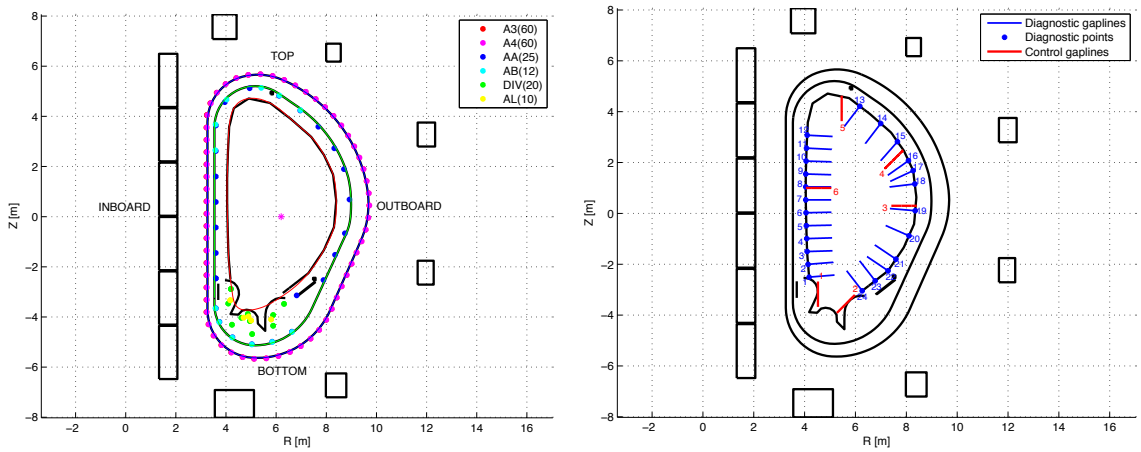

(a) (b)

Fig. 1: ITER machine cross section. (a) The geometry of the machine is shown, together with the poloidal field coils and the distribution of magnetic sensors. The real sensors are those highlighted with symbols, while the ideal observer is depicted as a continuous line in correspondence to the vacuum vessel border. (b) Shape descriptors: control gap-lines (in red) and diagnostics gap-points and lines (in blue).

An algorithm, the *Inverse Problem Tool (IPT)*, has been developed to support the magnetic analysis and sensor validation: It allows the reconstruction of the plasma boundary ($R-Z$ plane and polar coordinates) and of the plasma-first wall gaps using as input the measurements of the plasma equilibria [10][11]. More details are given in Sec. IV.

Moreover, to study the noise propagation from the sensor measurements to the boundary location, a simple model of the measurement noise has been adopted. For each sensor used as input to the reconstruction procedure, the noisy signal $\check{y}$ has been calculated adding to its actual value y two terms:

$$\check{y} = (1+\epsilon_r)\, y + \epsilon_a\, y_0, \tag{1}$$

where the measurement noise ϵ_r (normal distribution with zero mean and standard deviation σ_r) takes into account the errors proportional to the actual value of the signal, whilst the measurement noise ϵ_a (normal distribution with zero mean and standard deviation σ_a) takes into account the errors independent on the actual value , normalized to a typical field value $y_0 = 2.1\,T$. A balanced model with $\sigma_a = 0.35$ and $\sigma_r = 0.2$ appears realistic for the case of interest.

III. Statistical analysis of different sensor sets

The reconstruction capability of the magnetic sensors is studied through a statistical analysis based on the simulation data from a large set of equilibria, that include the different sensor sets and a set of virtual measurements. The focus is indeed the study of the statistical correlation between the set of measurements provided by the real sensors and the virtual measurements thought as a sort of *ideal observer*, similarly to what proposed for the JET machine during the magnetic enhancement project [12]. The rationale behind the ideal observer is that the magnetic signals along some closed contour outside the plasma (on the poloidal cross section) provides a description of the plasma shape and its configuration with respect to the active and passive circuits [13].

This analysis is not aiming at designing or optimizing the reconstruction technique but at assessing and comparing the behavior of different sensor sets: Therefore the results should be taken as a *relative* comparison, more than as an *absolute* performance. Nonetheless, this procedure can quantify the information brought in by the sensors, as far as the reconstruction capability is concerned.

In more detail, a sufficiently extended set of plasma configurations describing the operative space of ITER has been run (N_{eq} equilibria), to provide a dataset of real and virtual measurements. The correlation between the two sets of measurements is obtained by modeling a linear relation between the magnetic field on the virtual sensors and the data provided by the *real* (in the sense of *actually designed*) measurements.

In other words, each virtual magnetic measurement $\xi_i, i = 1, \ldots, N_{virt}$ can be singularly reconstructed from the real set measurements $\mathbf{y} = [y_j, j = 1, \ldots, N_{real}]^\top$ according to the following relation:

$$\hat{\xi}_i = \sum_{j=1}^{N_{real}} c_{ij} y_j = \mathbf{c}_i \cdot \mathbf{y}, \tag{2}$$

where $\hat{\xi}_i$ is the reconstructed virtual measurement, and the $\mathbf{c}_i$ coefficient vector can be obtained via least square fit (usually obtained by adding some regularization term, which corresponds to a linear combination of the most significant principal components) [14]. The norm of the reconstruction error, i.e. the difference (in norm) between the virtual measurement and that obtained by using the real sensors to reconstruct the field values in the same location, $\|\xi_i - \mathbf{c}_i \cdot \mathbf{y}\|$ states the performance of the real sensor set, namely the (specific) reconstruction capability.

At the same time, in the attempt to capture a general view of the reconstruction capability, a matrix can be obtained that summarizes the linear relation above, after having normalized in mean and variance all the available measurements (standard score) with respect to the plasma equilibria:

$$\tilde{\xi}_i = \frac{\xi_i - \bar{\xi}_i}{\sigma_{\xi_i}} \quad \text{and} \quad \tilde{y}_i = \frac{y_i - \bar{y}_i}{\sigma_{y_i}}. \tag{3}$$

This allows to equalize the dynamic range of the different sensors and introduce a numerical regularization over the datasets. The scalar relation (2) becomes $\tilde{\xi}_i \approx \tilde{\mathbf{c}}_i \cdot \tilde{\mathbf{y}}$: The real sensor measurements are organized into a matrix $\mathbf{Y} \in \mathbb{R}^{N_{real} * N_{eq}}$, where each row corresponds to a sensor and each column to an equilibrium, and similarly, $\mathbf{\Xi} \in \mathbb{R}^{N_{virt} * N_{eq}}$ is the matrix of the virtual measurements (magnetic field in the horizontal and vertical directions and flux differences between neighboring sensors), listing the various equilibria as columns:

$$\mathbf{Y} = \begin{bmatrix} \tilde{\mathbf{y}}_1 & \tilde{\mathbf{y}}_2 & \ldots & \tilde{\mathbf{y}}_{N_{eq}} \end{bmatrix} \tag{4}$$

$$\mathbf{\Xi} = \begin{bmatrix} \tilde{\boldsymbol{\xi}}_1 & \tilde{\boldsymbol{\xi}}_2 & \ldots & \tilde{\boldsymbol{\xi}}_{N_{eq}} \end{bmatrix}, \tag{5}$$

where clearly $\tilde{\boldsymbol{\xi}}_i$ refers to the whole virtual measurement vector. It follows:

$$\mathbf{\Xi} \approx \begin{bmatrix} \tilde{\mathbf{c}}_1 \\ \tilde{\mathbf{c}}_2 \\ \ldots \\ \tilde{\mathbf{c}}_{N_{virt}} \end{bmatrix} \cdot \begin{bmatrix} \tilde{\mathbf{y}}_1 & \tilde{\mathbf{y}}_2 & \ldots & \tilde{\mathbf{y}}_{N_{eq}} \end{bmatrix} = \mathbf{K} \cdot \mathbf{Y}, \tag{6}$$

where the matrix $\mathbf{K} \in \mathbb{R}^{N_{virt} * N_{real}}$ is named as *correlation matrix*. The study of the $\mathbf{K}$ matrix appears from these relations equivalent to the analysis of a transformation map between the space of the real measurements and that of the virtual ones.

More in detail, the computation of the $\mathbf{K}$ matrix is performed after a further pre-conditioning of the input signal matrices. In actual fact, a Singular Value Decomposition (SVD, [14]) is applied to both the real measurement space (represented by the $\mathbf{Y}$ matrix) and the virtual measurement space (represented by the $\mathbf{\Xi}$ matrix),

$$\mathbf{Y}^\top = \mathbf{U}_\mathbf{Y} \mathbf{S}_\mathbf{Y} \mathbf{V}_\mathbf{Y}^\top \quad \text{and} \quad \mathbf{\Xi}^\top = \mathbf{U}_\mathbf{\Xi} \mathbf{S}_\mathbf{\Xi} \mathbf{V}_\mathbf{\Xi}^\top \tag{7}$$

and a modified version of the $\mathbf{K}$ matrix is computed from the score matrices of $\mathbf{Y}^\top$ and $\mathbf{\Xi}^\top$ as

$$\mathbf{K}_{svd} \approx \left(\left(\mathbf{U}_\mathbf{Y} \mathbf{S}_\mathbf{Y} \right)^\dagger \left(\mathbf{U}_\mathbf{\Xi} \mathbf{S}_\mathbf{\Xi} \right) \right)^\top, \tag{8}$$

where $(\bullet)^\dagger$ indicates the Moore-Penrose pseudoinverse operator.

The reconstruction of the signal spaces is obtained retaining around the 99% of the energy of the signals, therefore in practice the information loss is negligible and well compensated by the beneficial effects of this procedure. Indeed, the numerical outcome of having reduced the correlation problem to the correlation between the principal components helps to regularize the solution and avoid the overfitting of specific singular equilibria, provided that in order to return a physically consistent result, the inverse mathematical transformations need also to be applied to obtain $\mathbf{K}$:

$$\mathbf{K} \approx \mathbf{V}_\mathbf{\Xi} \mathbf{K}_{svd} \mathbf{V}_\mathbf{Y}^\dagger. \tag{9}$$

IV. BOUNDARY RECONSTRUCTION

In addition, the solution to the inverse problem as a free boundary problem should also state a use-case for a possible implementation as a real-time diagnostics to be used in the control loop, to provide reference for the shape controller. Indeed, the non-feasibility of the use of numerical equilibrium codes for real-time boundary reconstruction, have pushed towards the derivation of alternative methods, based on simpler and faster numerical algorithms [15], such as *Equivalent Currents* [16], *Toroidal Harmonics* [17][18] or *Local Field Expansion* [19][20], which allow to comply with the specific requirements of the *on-line* plasma contour identification.

Actually, beyond the assessment of the diagnostics system, in this work a procedure aimed at the reconstruction of the plasma boundary and gaps based on Equivalent Currents is developed and validated against ITER reference equilibrium configurations.

At *steady state*, the N_{real} measurements $\mathbf{y}$ can be expressed as a linear combination of the n_c active coil currents $\mathbf{i}_c$ and the n_p plasma equivalent currents $\mathbf{i}_p$ effects

$$\mathbf{G}_c\,\mathbf{i}_c + \mathbf{G}_p\,\mathbf{i}_p = \mathbf{y}, \tag{10}$$

where the elements of the Green matrices $\mathbf{G}_c$, $\mathbf{G}_p$ are computed by means of a numerical integration using the standard closed formulas for the magnetic vector potential (flux loops and saddle coils) and flux density components (pick-up probes) produced by a unit axisymmetric current. For a given arrangement, the $\mathbf{i}_p$ values can be calculated from

$$\min_{\mathbf{i}_p} \|\mathbf{G}_p\mathbf{i}_p - \mathbf{y}_p\|_2 \tag{11}$$

where $\mathbf{y}_p = \mathbf{y} - \mathbf{G}_c\mathbf{i}_c$ represents the measurements $\mathbf{y}$ from which the known effect of the external coil currents $\mathbf{i}_c$ is subtracted, and $\|\cdot\|_2$ is the Euclidean norm. Being $N_{real} > n_p$, the numerical solution of (11) is ill-conditioned and a regularization method is needed to obtain a unique regular solution approximating the desired vector $\mathbf{y}_p$ [21]. The extent of the ill-conditioning is strongly dependent both on the probe locations (a crucial issue in the design of new machines) and on the arrangement selected for the equivalent currents. An SVD technique is usually adopted to approximate the ill-conditioned matrix $\mathbf{G}_p$ with a better-conditioned matrix.

By computing the singular value decomposition of the matrix $\mathbf{G}_p = \mathbf{U}\,\mathbf{S}\,\mathbf{V}^T$, being $\mathbf{S}$ the matrix of the singular values $s_i,\ i = 1, \ldots, k$ of $\mathbf{G}_p$ and $\mathbf{U}$, $\mathbf{V}$ orthogonal matrices, the solution vector can be expressed as

$$\mathbf{i}_p^{(k)} = \sum_{i=1}^{k} \frac{b_i}{s_i}\mathbf{v}_i \tag{12}$$

where $\mathbf{v}_i$ is the i-th column of $\mathbf{V}$; b_i is the i-th element of the vector $\mathbf{U}^T\,\mathbf{y}_p$; k is the truncation index usually selected such as $k < \min(N_{real}, n_p)$ in order to neglect the smaller singular values responsible for the ill-conditioning of $\mathbf{G}_p$.

As a matter of fact, it can be shown that the effect of the perturbation $\delta\mathbf{y}_p$ in the measurements propagates to the solution of (11) according to the relation

$$\frac{\|\delta\mathbf{i}_p\|}{\|\mathbf{i}_p\|} \leqq c(\mathbf{G}_p)\frac{\|\delta\mathbf{y}_p\|}{\|\mathbf{G}_p\|\,\|\mathbf{i}_p\|} \tag{13}$$

where the conditioning number $c(\mathbf{G}_p)$ of the system matrix $\mathbf{G}_p$ acts as an amplification factor with respect to the perturbations on the data.

In case of different sets of magnetic measurements (flux loops, saddle coils vs pick-up coils or inner vs outer probes), a key role is played by the different levels of measurement noise (e.g. standard deviations σ_i) which can be accounted for by the pre-multiplication of the residual vector in (11) by the diagonal matrix of the standard deviations $\Sigma = diag(\sigma_i)$

$$\min_{\mathbf{i}_p} \|(\Sigma\mathbf{G}_p)\mathbf{i}_p - \Sigma\mathbf{y}_p\|_2 \tag{14}$$

Among the several alternative distributions of equivalent current filaments, a limited set has been analyzed and the choice of the model for the magnetic assessment has relies on the capability of the filament set to better relate to the magnetic measurements. This calculation has involved the computation of the eigenvalues of a map between the currents and the measurements: The larger the eigenvalues, the stronger the relation between the two sets of quantities (Fig. 2).

The *IPT* algorithm is then summarized as follows:

- a set of n_p axisymmetric equivalent currents $\mathbf{i}_p$ are distributed along an ellipse centered in the plasma centroid;
- the known term $\mathbf{y}_p$ is calculated by subtracting the contribution of the external coil currents from the measurements;
- the values of the equivalent currents $\mathbf{i}_p$ are calculated from the solution of (14)
- the flux value of the plasma boundary is evaluated by means of the linear combination of the plasma equivalent currents $\mathbf{i}_p$ and active coils $\mathbf{i}_c$ contributions;
- finally, the plasma boundary and the gaps are reconstructed.

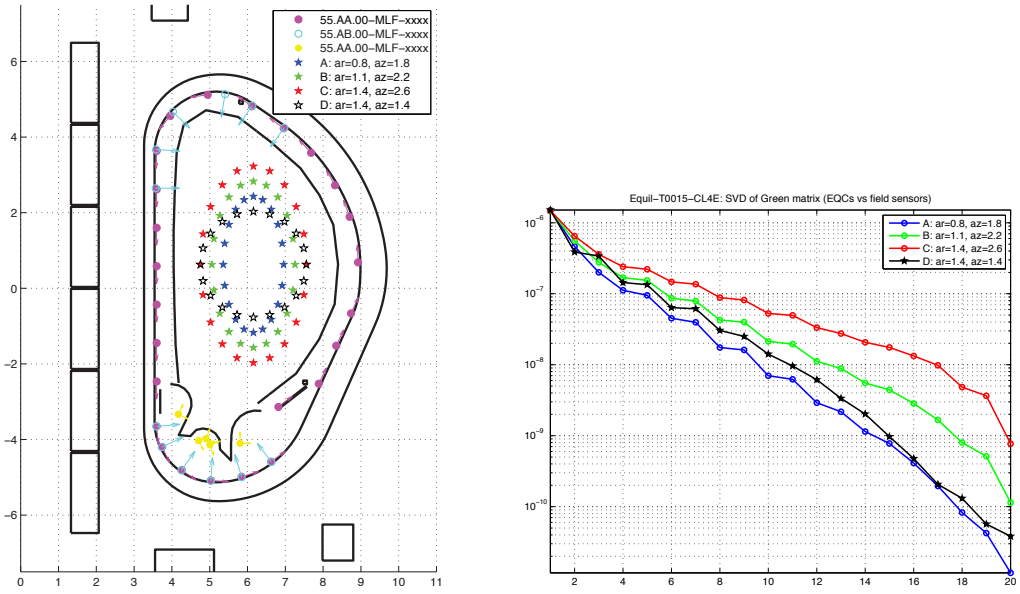

(a) (b)

Fig. 2: Filamentary plasma model. (a) The positions of different plasma filamentary models are shown. (b) The analysis of the eigenvalues of these arrangements with respect to a set of measurements suggests the employment of the set highlighted in red.

V. Discussion and Results

The statistical analysis provides a twofold insight into the reconstruction capability of the diagnostics and the assessment for their use for real-time estimation of the boundary location, by examining the $\mathbf{K}$ matrix either from the observer point of view (i.e. combining the row entries to obtain a N_{virt}-dimensional vector) or from the real measurements perspective (i.e. combining the column entries to obtain a N_{real}-dimensional vector).

In the former case, the sensitivity of the reconstruction of the field components all around the plasma (the virtual measurements) is inferred with respect to all the available measurements. The interpretation of these results is in terms of *what effort* the reconstruction of the magnetic field requires: The lower the effort, the higher the overall noise reduction and the avoidance of a potentially dangerous excessive sensitivity (Fig. 3). In actual fact, this result is well confirmed by numerical simulation with the IPT, in which the noise model (1) is applied to the magnetic sensors to measure how this affects the reconstruction of the plasma boundary position.

On the other hand, the indication of how much a specific real signal contributes to the reconstruction of the field in a particular location (participation factor) states the significance of the rôle of the specific sensor in reconstructing the field, and hence the boundary position and shape. An example of the contribution factors of two different set of sensors is given in Fig. 4.

In this sense, some comments are in order:

- an ideal sensor set should equally share the burden of the reconstruction, meaning that all the contribution factors should stay approximately in a narrow range of values: In other words, the more the contribution are equal, the more the set is able compensate for sensor loss or faulty measurements;
- the presence of peaks in the sensor contributions suggests that the reconstruction is strongly dependent on those specific measurements;
- the presence of alternating contributions (i.e. high-low-high-low and so on) in neighboring sensors highlights a certain level of redundancy in the set;
- by exploiting more sensor measurements, the contributions of the real signals is reduced by sharing the reconstruction task among a larger amount of diagnostics: Broadly speaking, this results in an improved robustness and noise rejection as the whole system is less dependent on single measurements.

This statistical analysis is further corroborated by numerical simulations of specific equilibria with the IPT tool. Different sets of sensors are employed in the boundary reconstruction algorithm, where the most (Set 1A) or the least contributing (Set 1B) magnetic measurements are respectively neglected in the reconstruction. The Mean Square Error (MSE) on the gap reconstructions is computed and shown in Tab. I.

In general, as shown in these cases, the reconstruction of Set 1A is better than Set 1B, as expected since we are removing in one case the most contributing sensors while in the other the least contributing ones; more interestingly, the reconstruction

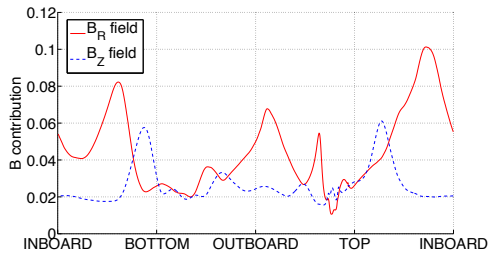

(a)

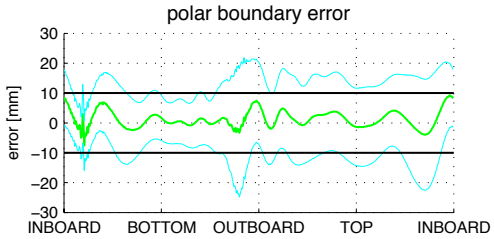

(b)

Fig. 3: Sensitivity of the ideal observer. The sensitivity of the magnetic field reconstruction (a) is well in agreement with the simulations of noise propagation from the sensors to the boundary location for a plasma configuration (here the result for a diverted configuration is shown) (b).

TABLE I: Boundary reconstruction on selected equilibria.

	MSE - control gaps			MSE - diagnostic gaps		
Equilibrium	Set1	Set 1A	Set 1B	Set 1	Set 1A	Set 1B
Eq. 015	1.26	2.28	1.87	1.72	3.20	1.49
Eq. 066	0.59	1.15	0.58	0.80	1.79	0.51
Eq. 230	0.79	4.18	0.88	1.81	4.88	2.05
Eq. 339	0.73	0.83	0.78	0.40	1.22	0.49

is always less accurate when using Set 1A than when using the original Set 1, meaning that the *important* sensors are actually effective in the reconstructions; conversely, in some case, removing some measurements can have a beneficial effect in the reconstruction: This effect can be related in part to the statistical selection of the signals, which refers to the whole equilibrium set of interest.

By fusing the information from this analysis, the most important sensors in the magnetics result (see Fig. 5).

VI. Conclusion

In this work the problem of diagnostic system assessment for plasma boundary reconstruction has been addressed.

A statistical procedure has been proposed to quantify the information brought in by different sensor sets, as far as the reconstruction capability is concerned. This procedure is based on the definition of an ideal observer, namely a dense array of virtual sensors measuring all the magnetic field components placed outside but close to the plasma so as to capture its magnetic configuration. The analysis of the transformation map between the real sensor measurements and the virtual measurements obtained from a large number of plasma equilibria allows to infer on the one side the sensitivity of the field (and boundary) reconstruction on measurement noise, while on the other the contribution of each real measurement to the reconstruction, hence its importance. Moreover, starting from these sensor sets, an algorithm for the boundary shape estimation has been devised, that represents the first step towards the definition of a real-time code for plasma boundary reconstruction which is mandatory for shape control and shape optimization during the experiment.

Both the assessment strategy and the reconstruction algorithm have been cross validated through numerical simulations.

References

[1] R. Albanese, J. Blum, and O. De Barbieri, Numerical studies of the next European torus via the PROTEUS Code, in Proc. 12th Conf. Numeri- cal Simulation of Plasmas, S. Francisco, CA, 1987, paper IT4, pp. 12.

[2] A. Beghi, A. Cenedese, Advances in real-time plasma boundary reconstruction: From gaps to snakes, IEEE Control Systems Magazine, vol. 25(5), pp. 44–64, 2005.

[3] V. Coccorese, R. Albanese, H. Altmann, *et al.*, Design of the new magnetic sensors for Joint European Torus, Review of Scientific Instruments, vol. 75, pp. 4311–4313, 2004.

[4] V. Coccorese, G. Artaserse, G. Chitarin, *et al.*, Assessment of new ex-vessel magnetic measurements in JET, Review of Scientific Instruments, vol. 77, pp. 10E317, 2006.

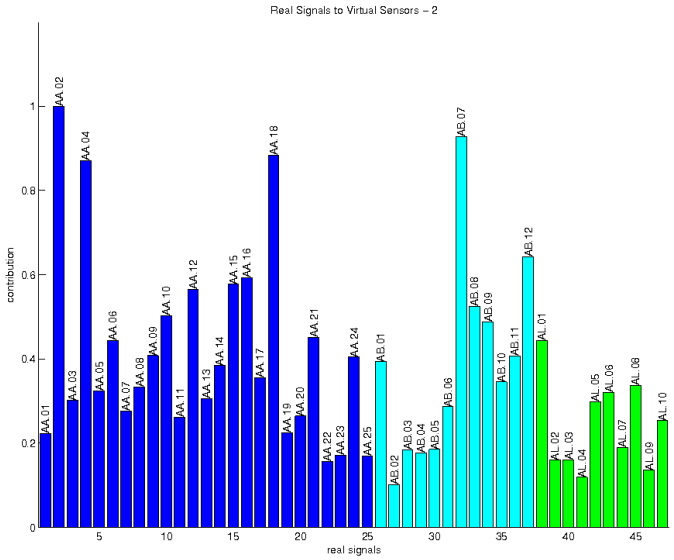

(a) Set 1

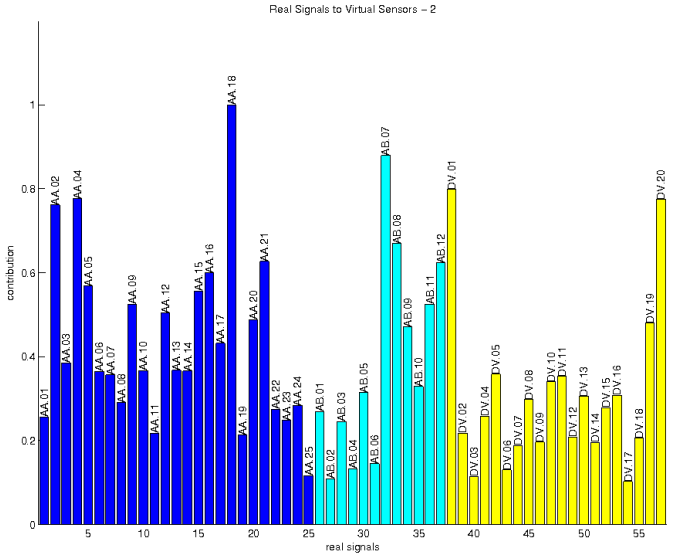

(b) Set 2

Fig. 4: Contribution factors of two different sets to the reconstruction of the ideal observer (see Fig. 1(a)).

[5] J.L. Luxon and B.B. Brown, Magnetic analysis of non-circular cross-section tokamaks, Nuclear Fusion, vol. 22(6), pp. 813–822, 1982.

[6] L.L. Lao, H. St.John, R.D. Stambaugh, *et al.*, Reconstruction of current profile parameters and plasma shapes in tokamaks, Nuclear Fusion, vol. 25(11), pp. 1611–, 1985.

[7] J. Blum, J. Le Foll, B. Thooris, The self-consistent equilibrium and diffusion code SCED, Comp. Phys. Communications, vol. 24(3–4), pp. 235–254, 1981.

[8] L.L. Lao, J.R. Ferron, R.J. Groebner, *et al.*, Equilibrium analysis of current profiles in tokamaks, Nuclear Fusion, vol. 30(6), pp. 1035–1050, 1990.

[9] J.R. Ferron, M.L. Walker, L.L. Lao, *et al.*, Real time equilibrium reconstruction for tokamak discharge control, Nuclear Fusion, vol. 38(7), pp. 1055–1067, 1998.

[10] P. Bettini, A. Formisano, R. Martone, *et al.*, Identification of the plasma magnetic contour from external magnetic measurements by means of equivalent currents, European Physical Journal of Applied Physics, vol. 13, pp. 51–57, 2001.

[11] P. Bettini, A. Formisano, R. Martone, *et al.*, Combined reconstruction techniques for geometrical and magnetic characteristics of thermonuclear plasmas, COMPEL, vol. 20, pp. 699–712, 2001.

[12] A. Cenedese, R. Albanese, G. Artaserse, *et al.*, Reconstruction capability of JET magnetic sensors, Fusion Engineering and Design, vol. 74, pp. 825–830, 2005.

[13] I.P. Shkarofsky, Evaluation of multipole moments over the current density in a tokamak with magnetic probes, Physics of Fluids, vol. 25(1), pp. 89-96, 1982.

[14] T.W. Anderson, An Introduction to Multivariate Statistical Analysis, John Wiley & Sons, Inc., 2003.

[15] L.C.J.M. De Kock and Yu.K. Kuznetsov, Magnetic diagnostics for fusion plasmas, Nuclear Fusion, vol. 36(3), pp. 387–, 1996.

[16] D.W. Swain and G.H. Neilson, An efficient technique for magnetic analysis of non-circular, high-beta tokamak equilibria, Nuclear Fusion, vol. 22(8), pp. 1015–1031, 1982.

[17] D.K. Lee, Y.K.M. Peng, An approach to rapid plasma shape diagnostics in tokamaks, J. Plasma Physics, vol. 25(1), pp. 161-173, 1981.

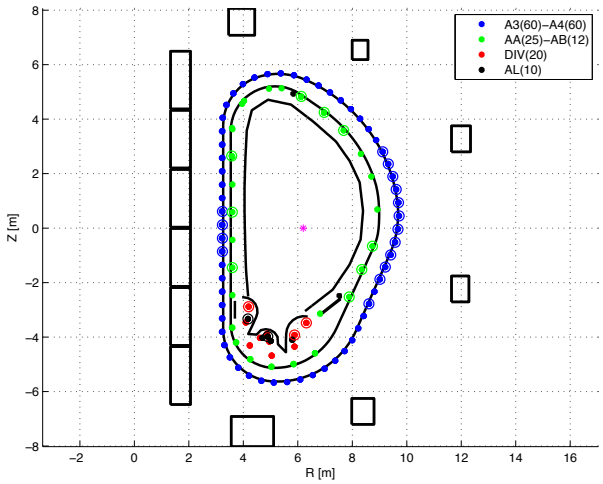

Fig. 5: ITER most important sensors. The most contributing magnetic diagnostics among the considered sets are shown with larger markers.

[18] F. Alladio and F. Crisanti, Analysis of MHD equilibria by toroidal multipolar expansions, Nuclear Fusion, vol. 26(9), pp. 1143–1165, 1986.
[19] A. Cenedese, F. Sartori and M. Macuglia, Development of fixed-position filamentary plasma model based on the current moment description, IEE Proc.-Sci. Meas. Technol., vol. 151, pp. 484–487, 2004.
[20] L. Zabeo, G. Artaserse, A. Cenedese, F. Piccolo, F. Sartori, A new approach to the solution of the vacuum magnetic problem in fusion machines, Fusion Engineering and Design, vol. 82, pp. 1081–1088, 2007.
[21] C.L. Lawson, R.J. Hanson, Solving Least Squares Problems, Prentice-Hall, 1974.